

Lattice QCD calculation of the electroweak box diagrams for the kaon semileptonic decays

Peng-Xiang Ma,¹ Xu Feng,^{1,2,3,*} Mikhail Gorchtein,^{4,5,6,†}

Lu-Chang Jin,^{7,8,‡} and Chien-Yeah Seng^{9,§}

¹*School of Physics and State Key Laboratory of Nuclear Physics and Technology, Peking University, Beijing 100871, China*

²*Collaborative Innovation Center of Quantum Matter, Beijing 100871, China*

³*Center for High Energy Physics, Peking University, Beijing 100871, China*

⁴*Helmholtz Institute Mainz, Mainz, Germany*

⁵*GSI Helmholtzzentrum für Schwerionenforschung, Darmstadt, Germany*

⁶*Johannes Gutenberg University, Mainz, Germany*

⁷*Department of Physics, University of Connecticut, Storrs, CT 06269, USA*

⁸*RIKEN-BNL Research Center, Brookhaven National Laboratory, Building 510, Upton, NY 11973*

⁹*Helmholtz-Institut für Strahlen- und Kernphysik and Bethe Center for Theoretical Physics, Universität Bonn, 53115 Bonn, Germany*

(Dated: February 25, 2021)

Abstract

We present a lattice QCD calculation of the axial γW -box diagrams relevant for the kaon semileptonic decays. We utilize a recently proposed method, which connects the electroweak radiative corrections in Sirlin's representation to that in chiral perturbation theory. It allows us to use the axial γW -box correction in the SU(3) limit to obtain the low energy constants for chiral perturbation theory. From first principles our results confirm the previously used low energy constants provided by the minimal resonance model with a significant reduction in uncertainties.

* xu.feng@pku.edu.cn

† gorshtey@uni-mainz.de

‡ ljin.luchang@gmail.com

§ cseng@hiskp.uni-bonn.de

I. INTRODUCTION

In the Standard Model, the Cabibbo-Kobayashi-Maskawa (CKM) matrix is a three-generation quark mixing matrix which describes how the strength of the flavour-changing weak interaction in the leptonic sector is distributed among the three quark generations. The precise determination of the CKM matrix elements is of vital importance in the stringent test of CKM unitarity and search of new physics beyond the Standard Model. As quoted in the 2020 Review by the Particle Data Group [1], there exists a ~ 3 sigma deviation from unitarity in the first row of CKM matrix elements

$$|V_{ud}|^2 + |V_{us}|^2 + |V_{ub}|^2 = 0.9984(3)_{V_{ud}}(4)_{V_{us}}. \quad (1)$$

Here $|V_{ub}|^2 \approx 1.5 \times 10^{-5}$ is negligibly small and thus only $|V_{ud}|$ and $|V_{us}|$ play a role in the unitarity test.

The most precise determination of $|V_{ud}| = 0.97370(10)_{\text{exp+nucl}}(10)_{\text{RC}}$ quoted in the 2020 PDG review [1] stems from the superallowed nuclear beta decays [2, 3], with the first uncertainty arising from the experimental measurements and nuclear physics corrections and the second one from the electroweak radiative corrections (RCs)¹. It is the update of the RCs from a dispersive analysis [4, 6], which makes the value of $|V_{ud}|$ about 2σ smaller than that in the 2018 PDG review [7]. Very recently, the RCs to the $\pi_{\ell 3}$ decays were calculated using lattice QCD with the focus on the so-called axial γW -box diagrams [8]. It allowed for a significant reduction of the hadronic uncertainty in the RCs, and provided an independent cross-check of the dispersion relation analysis of the neutron RCs [9]. In the future a direct lattice QCD calculation of the RCs to the neutron decay could help to further improve the determination of $|V_{ud}|$ [10].

The $|V_{us}|$ can be determined from kaon, hyperon or tau decays, with kaon decays providing the best precision. Leptonic decays $K \rightarrow \mu\nu$ (denoted by $K_{\mu 2}$) combined with $\pi \rightarrow \mu\nu$ give access to the ratio $|V_{us}/V_{ud}|$, whereas semileptonic decays $K \rightarrow \pi\ell\nu$ (denoted by $K_{\ell 3}$) give a handle on $|V_{us}|$ independently. The traditional way of determining $|V_{us}|$ relies on the experimental measurements of $K_L^0 \rightarrow \pi e\nu$ to avoid the isospin-breaking effects (π^0 - η mixing) in the charged kaon decays and the complication from the second (scalar) form

¹ Notice, however, that this quoted value does not include the contributions from several new nuclear corrections investigated in Refs.[4, 5].

factor present in the muonic decays. Nowadays, due to the high-statistics data collected in the experiments, the comparison between different decay modes is justified [11]. The decays including $K_L^0 \rightarrow \pi \ell \nu$, $K^\pm \rightarrow \pi^0 \ell^\pm \nu$ and $K_S^0 \rightarrow \pi e \nu$ with $\ell = e, \mu$ are used to determine $|V_{us}|$ via the master formula [1]

$$\Gamma_{K\ell 3} = \frac{G_F^2 m_K^5}{192\pi^3} S_{EW} (1 + \delta_K^\ell + \delta_{SU2}) C^2 |V_{us}|^2 f_+^2(0) I_K^\ell. \quad (2)$$

Here, $\Gamma_{K\ell 3}$ is the $K_{\ell 3}$ decay width, G_F is the Fermi constant, m_K is the kaon mass, S_{EW} is the short-distance radiative correction, δ_K^ℓ is the long-distance radiative correction, δ_{SU2} is the strong isospin-violating effect, C^2 is 1 for the neutral kaon decay and 1/2 for the charged case, $f_+(q^2)$ is the $K^0 \rightarrow \pi^-$ vector form factor and I_K^ℓ is the phase-space integral which contains the information of the momentum dependence in the form factors. Averaging over the experimental measurements with appropriate theory inputs of various Standard Model corrections, the product $|V_{us}|f_+(0)$ is given as [12]

$$f_+(0)|V_{us}| = 0.2165(4), \quad (3)$$

with the uncertainty dominated by the experimental measurements and RCs. The form factor $f_+(0)$ can be provided by lattice QCD calculations [13–17]. The FLAG average [18] for $N_f = 2 + 1 + 1$ simulations yields $f_+(0) = 0.9698(17)$ according to an update on December 2020, which results in a determination of

$$|V_{us}| = 0.2232(4)_{\text{exp+RC}}(4)_{\text{lat}}, \quad \text{for } K_{\ell 3}. \quad (4)$$

High-precision experimental data on $K_{\mu 2}$ and $\pi_{\mu 2}$ decays [19, 20] also accurately determine the ratio $|V_{us}/V_{ud}|f_{K^\pm}/f_{\pi^\pm} = 0.2760(4)$ [12]. Employing the FLAG $N_f = 2 + 1 + 1$ lattice QCD average [21–24] for the ratio of decay constants $f_{K^\pm}/f_{\pi^\pm} = 1.1932(21)$, a value of $|V_{us}| = 0.2252(5)$ is obtained, which has a 2.6σ deviation from the $K_{\ell 3}$ -based value. Combining the $|V_{us}|$ from $K_{\ell 3}$ and $K_{\mu 2}$ decays yield ²

$$|V_{us}| = 0.2243(8), \quad \text{weighted average of } K_{\ell 3} \text{ and } K_{\mu 2}. \quad (5)$$

It should also be mentioned that $|V_{us}|$ obtained from hyperon and tau decays are given by $|V_{us}| = 0.2250(27)$ [25] and $0.2221(13)$ [26], respectively, both having larger uncertainties than the kaon decays.

² Here $|V_{us}|$ is slightly different from the PDG value $0.2245(8)$ due to the update of the FLAG value of $f_+(0)$. Correspondingly, the value of $|V_{ud}|^2 + |V_{us}|^2 + |V_{ub}|^2$ given in Eq. (1) also slightly differs from the PDG value of $0.9985(3)_{V_{ud}}(4)_{V_{us}}$.

To gain a better understanding of the violation of the first-row CKM unitarity in Eq. (1) and the disagreement in the determination of $|V_{us}|$ between the $K_{\ell 3}$ and $K_{\mu 2}$, for the $K_{\ell 3}$ decays it requires both a more precise determination of the form factor $f_+(0)$ and a direct calculation of RCs from lattice QCD. The latter is more challenging due to the inclusion of both weak and electromagnetic currents in the calculation and is the focus in this paper.

Recently, the horizons of lattice QCD studies have been extended to include various processes with higher-order electroweak interactions. The examples include kaon mixing [27–29], rare kaon decays [30–35], double beta decays [36–44], inclusive B -meson decays [45–47], as well as the electromagnetic and radiative corrections to the weak decays [48–54]. Among all these processes, the lattice QCD calculation of RCs in $K_{\ell 3}$ still remains one of the largest challenges as it essentially involves a computation of five-point correlation functions. In Ref. [55], it proposes a new method which bridges the lattice QCD calculation with chiral perturbation theory (ChPT) [56, 57]. For the $K_{\ell 3}$ decay in the flavor SU(3) limit, it demonstrates that the lattice QCD calculation of the axial γW -box diagrams can provide all unknown low-energy constants (LECs) that enter the long-distance radiative correction δ_K^ℓ in the ChPT representation at the order of $O(e^2 p^2)$, thus removing the dependence of the RCs on the model used to estimate these LECs. In this paper we will first briefly introduce the methodology and then present the lattice calculation of RCs.

II. METHODOLOGY

We start the discussion of the treatment of RCs in $K_{\ell 3}$ decays with two theoretical frameworks: Sirlin’s representation and the ChPT representation.

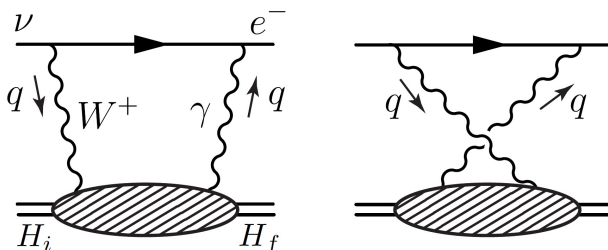


Figure 1. The γW -box diagrams for the semileptonic decay process $H_i \rightarrow H_f e \bar{\nu}_e$.

Sirlin’s representation is particularly useful in the treatment of the semileptonic decay $H_i \rightarrow H_f e \bar{\nu}_e$ with the hadrons H_i and H_f having nearly the same masses $m_i \approx m_f$. In this

case, the $O(G_F\alpha_e)$ RCs to the decay width is given as [58]

$$\delta = \frac{\alpha_e}{2\pi} \left[\bar{g} + 3 \ln \frac{m_Z}{m_p} + \ln \frac{m_Z}{m_W} + \tilde{a}_g \right] + \delta_{\text{HO}}^{\text{QED}} + 2\Box_{\gamma W}^{VA}, \quad (6)$$

where m_Z and m_W are the masses for the Z and W bosons. m_p is the proton mass that enters simply by convention. The Sirlin's function \bar{g} , which is a function of the electron's end-point energy, summarizes the infrared-singular contributions involving both the one-loop and bremsstrahlung corrections [58–60]. The $O(\alpha_s)$ QCD correction \tilde{a}_g is dominated by the high-energy scale $Q^2 \simeq m_W^2$ with a relatively small contribution of $\frac{\alpha_e}{2\pi}\tilde{a}_g \approx -9.6 \times 10^{-5}$ [58, 61]. The contribution from the resummation of the large QED logs is contained in $\delta_{\text{HO}}^{\text{QED}} = 0.0010(3)$ [62]. All the contributions that are sensitive to hadronic scales, reside in the axial γW -box contribution $\Box_{\gamma W}^{VA}$, as shown in Fig. 1. The total contribution δ is equivalent to $(S_{EW} - 1) + \delta_K^e$ shown in Eq. (2).

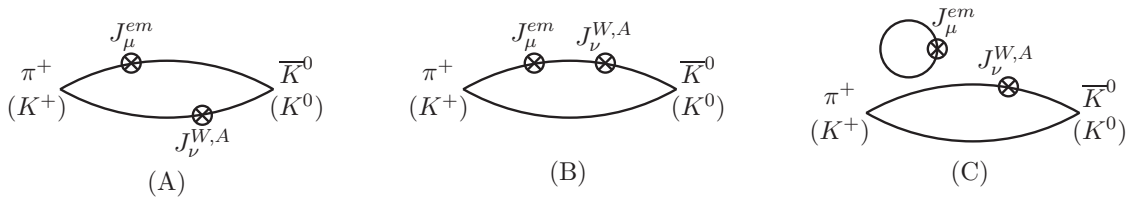


Figure 2. Quark contractions for $\bar{K}^0 \rightarrow \pi^+ e \bar{\nu}_e$ and $K^0 \rightarrow K^+ e \bar{\nu}_e$.

In the $K_{\ell 3}$ decays, since m_K is not close to m_π , the non-perturbative hadronic effects are contained not only in $\Box_{\gamma W}^{VA}$, but also in other diagrams. As a consequence, Eq. (6) can not be used directly. To evaluate the total RCs, the calculation of the five-point correlation function is required. To simplify this problem, Ref. [55] proposes to calculate the RCs for $\bar{K}^0 \rightarrow \pi^+ e \bar{\nu}_e$ in the flavor SU(3) limit, where $m_K = m_\pi$. The relevant contractions are shown in Fig. 2 with the disconnected diagram (C) vanishing in the flavor SU(3) limit. Although the physical value of δ cannot be determined directly using this unphysical setup, the lattice calculation can help to extract the LECs for ChPT. Then by using ChPT one can obtain the physical RCs. Besides for the $\bar{K}^0 \rightarrow \pi^+$ transition, the semileptonic decay of $K^0 \rightarrow K^+ e \bar{\nu}_e$ can also be used to determine the same LECs as it has the same contractions as $\bar{K}^0 \rightarrow \pi^+$ up to the disconnected parts.

In ChPT, the RCs to $K_{\ell 3}$ are computed to $O(e^2 p^2)$ [56, 57, 63] with the short-distance

radiative correction

$$S_{EW} = 1 - e^2 \left[-\frac{1}{2\pi^2} \ln \frac{M_Z}{M_\rho} + (X_6^{\text{phys}})_{\alpha_s} \right] + \delta_{\text{HO}}^{\text{QED}} = 1.0229(3), \quad (7)$$

where $M_\rho = 0.77$ GeV is the rho mass and $(X_6^{\text{phys}})_{\alpha_s} \approx 3.0 \times 10^{-3}$ [64] summarizes the $O(\alpha_s)$ pQCD contribution to X_6^{phys} with $X_6^{\text{phys}}(\mu) \equiv X_6^r(\mu) - 4K_{12}^r(\mu)$ the combination of two renormalized LECs. The scale μ is usually taken as $\mu = M_\rho$ in the numerical analysis. The long-distance radiative correction δ_K^ℓ has the dependence on the LECs through the relation³

$$\begin{aligned} \delta_{K^\pm}^\ell &= 2e^2 \left[-\frac{8}{3}X_1 - \frac{1}{2}\tilde{X}_6^{\text{phys}}(M_\rho) \right] + \dots \\ \delta_{K^0}^\ell &= 2e^2 \left[\frac{4}{3}X_1 - \frac{1}{2}\tilde{X}_6^{\text{phys}}(M_\rho) \right] + \dots, \end{aligned} \quad (8)$$

where the ellipses indicates the omission of the known kinematic terms, which does not depend on the LECs. X_1 and $\tilde{X}_6^{\text{phys}}$ are LECs relevant at $O(e^2 p^2)$. $\tilde{X}_6^{\text{phys}}(M_\rho) \equiv X_6^{\text{phys}}(M_\rho) + (2\pi^2)^{-1} \ln(M_Z/M_\rho) - (X_6^{\text{phys}})_{\alpha_s}$ removes the large electroweak logarithm and the $O(\alpha_s)$ pQCD correction from X_6^{phys} . In a similar way, one can define the quantity $\delta_{\pi^\pm}^\ell$ for $\pi_{\ell 3}$

$$\delta_{\pi^\pm}^\ell = 2e^2 \left[-\frac{2}{3}X_1 - \frac{1}{2}\tilde{X}_6^{\text{phys}}(M_\rho) \right] + \dots. \quad (9)$$

Since the neutral kaon decay mode $\bar{K}^0 \rightarrow \pi^+ e \bar{\nu}_e$ is theoretically cleaner as it does not receive contributions from the π^0 - η mixing which complicates the analysis in the flavor SU(3) limit, we may use it to extract the LECs. Comparing the ChPT and Sirlin's representations, the relation between the axial γW -box contribution $\square_{\gamma W}^{VA}|_{K^0, \text{SU}(3)}$ and the LECs is given by [55]

$$-\frac{8}{3}X_1 + \bar{X}_6^{\text{phys}}(M_\rho) = -\frac{1}{2\pi\alpha} \left(\square_{\gamma W}^{VA}|_{K^0, \text{SU}(3)} - \frac{\alpha}{8\pi} \ln \frac{M_W^2}{M_\rho^2} \right) + \frac{1}{8\pi^2} \left(\frac{5}{4} - \tilde{a}_g \right). \quad (10)$$

with $\bar{X}_6^{\text{phys}}(M_\rho)$ defined as $\bar{X}_6^{\text{phys}}(M_\rho) \equiv X_6^{\text{phys}}(M_\rho) + (2\pi^2)^{-1} \ln(M_Z/M_\rho)$, which removes only the large electroweak logarithm but retains the full pQCD corrections. For the $\pi_{\ell 3}$ decay, the relation is given by

$$\frac{4}{3}X_1 + \bar{X}_6^{\text{phys}}(M_\rho) = -\frac{1}{2\pi\alpha} \left(\square_{\gamma W}^{VA}|_\pi - \frac{\alpha}{8\pi} \ln \frac{M_W^2}{M_\rho^2} \right) + \frac{1}{8\pi^2} \left(\frac{5}{4} - \tilde{a}_g \right). \quad (11)$$

³ Notice that in a similar expression in Ref. [55], the quantity $\delta_{K^\pm}^\ell$ includes also contributions from the LECs $\{K_i^r\}$. That, however, was not the standard convention adopted by the ChPT community, which chooses to lump the $\{K_i^r\}$ contribution into δ_{SU2} .

The box contribution $\square_{\gamma W}^{VA}|_{\pi}$ for the $\pi_{\ell 3}$ decay has been calculated in Ref. [8]. The focus of this paper is on the determination of $\square_{\gamma W}^{VA}|_{K^0, \text{SU}(3)}$, from which the LECs X_1 and $\bar{X}_6^{\text{phys}}(M_\rho)$ can be obtained.

The lattice QCD calculation of $\square_{\gamma W}^{VA}|_{K^0, \text{SU}(3)}$ can follow the procedures given in Ref. [8]. We first define the hadronic function $\mathcal{H}_{\mu\nu}^{VA}(t, \vec{x})$ in Euclidean space

$$\mathcal{H}_{\mu\nu}^{VA}(t, \vec{x}) \equiv \langle \pi^+(P) | T [J_\mu^{em}(t, \vec{x}) J_\nu^{W,A}(0)] | \bar{K}^0(P) \rangle, \quad (12)$$

where $J_\mu^{em} = \frac{2}{3}\bar{u}\gamma_\mu u - \frac{1}{3}\bar{d}\gamma_\mu d - \frac{1}{3}\bar{s}\gamma_\mu s$ is the electromagnetic quark current, and $J_\nu^{W,A} = \bar{u}\gamma_\nu\gamma_5 s$ is the axial part of the weak charged current. The Euclidean momentum P is chosen as $P = (im_K, \vec{0})$ with $m_K = m_\pi$ in the flavor SU(3) limit. The box contribution $\square_{\gamma W}^{VA}|_{K^0, \text{SU}(3)}$ can be determined through the integral

$$\square_{\gamma W}^{VA}|_{K^0, \text{SU}(3)} = \frac{3\alpha_e}{2\pi} \int \frac{dQ^2}{Q^2} \frac{m_W^2}{m_W^2 + Q^2} M_K(Q^2) \quad (13)$$

with

$$M_K(Q^2) = -\frac{1}{6} \frac{\sqrt{Q^2}}{m_K} \int d^4x \omega(t, \vec{x}) \epsilon_{\mu\nu\alpha 0} x_\alpha \mathcal{H}_{\mu\nu}^{VA}(t, \vec{x}),$$

$$\omega(t, \vec{x}) = \int_{-\frac{\pi}{2}}^{\frac{\pi}{2}} \frac{\cos^3 \theta d\theta}{\pi} \frac{j_1(\sqrt{Q^2}|\vec{x}|\cos\theta)}{|\vec{x}|} \cos(\sqrt{Q^2}t \sin\theta). \quad (14)$$

Here $j_1(x)$ is the spherical Bessel function. To compute the integral in Eq. (13), for small Q^2 , we use lattice QCD input of $\mathcal{H}_{\mu\nu}^{VA}(t, \vec{x})$. For large Q^2 , the operator product expansion of $J_\mu^{em}(x) J_\nu^{W,A}(0)$ is utilized with the Wilson coefficients given at the four-loop accuracy [65, 66]. For more details, we refer the readers to Ref. [8].

III. NUMERICAL RESULTS

Five gauge ensemble with $N_f = 2+1$ -flavor domain wall fermion are used in the calculation. The detailed information is shown in Table I. Here 48I and 64I use the Iwasaki gauge action in the simulation (denoted as Iwasaki) while the other three ensembles use Iwasaki+DSDR action (denoted as DSDR). We place the Coulomb gauge-fixed wall-source quark propagators on all time slices. We calculate point-source propagators at $O(1000)$ random spacetime locations. The correlation functions are constructed using the field sparsening technique [67, 68] with a significant reduction in the propagator storage. For the locations of two current

Ensemble	m_π [MeV]	L	T	a^{-1} [GeV]	
24D	141.2(4)	24	64	1.015	
DSDR	32D	141.4(3)	32	64	1.015
	32D-fine	143.0(3)	32	64	1.378
Iwasaki	48I	135.5(4)	48	96	1.730
	64I	135.3(2)	64	128	2.359

Table I. Ensembles used in this work. For each ensemble we list the pion mass m_π , the spatial and temporal extents, L and T , the inverse of lattice spacing a^{-1} .

insertions J_μ^{em} and $J_\nu^{W,A}$, we treat one as the source of the propagator and the other as the sink. In this way the hadronic function $\mathcal{H}_{\mu\nu}^{VA}(t, \vec{x})$, which depends on the coordinate-space variable x can be obtained. Such technique has also been used in the computation of three-point correction function to extract the pion charge radius [69]. The flavor SU(3) limit is achieved by tuning down the strange quark mass to be the same as the light quark mass.

Inserting $\mathcal{H}_{\mu\nu}^{VA}(t, \vec{x})$ into the integral (14), we calculate the scalar function $M_K(Q^2)$. The lattice results for $M_K(Q^2)$ as a function of Q^2 are shown in the left panel of Fig. 3. At large Q^2 ($Q^2 \gtrsim 1 \text{ GeV}^2$), the lattice results from different gauge ensembles start to disagree, suggesting the obvious lattice discretization effects. In the right panel of Fig. 3, a continuum extrapolation is performed to obtain the results in the continuum limit for Iwasaki and DSDR ensembles separately. To reduce the systematic uncertainties contained in the lattice data at large Q^2 , we calculate the $M_K(Q^2)$ in pQCD using the RunDec package [70]. At low Q^2 the perturbative results suffer from large pQCD truncation effects due to the lack of higher-loop and higher-twist contributions. We observe an expected discrepancy between the orange and magenta curves at low Q^2 , where the former uses the 4-flavor theory down to 1 GeV, while the latter turns to the 3-flavor theory upon decoupling the charm quark at 1.6 GeV.

We introduce a momentum-squared scale Q_{cut}^2 that separates the Q^2 -integral into two regimes. We use the lattice data to determine the integral for $Q^2 \leq Q_{\text{cut}}^2$ and perturbation theory to determine the integral for $Q^2 > Q_{\text{cut}}^2$. Three values of $Q_{\text{cut}}^2 = 1, 2, 3 \text{ GeV}^2$ are used to check the Q_{cut}^2 -dependence in the final results. The corresponding results for $\square_{\gamma W}^{VA, \leq} \Big|_{K^0, \text{SU}(3)}$ and $\square_{\gamma W}^{VA, >} \Big|_{K^0, \text{SU}(3)}$ are listed in Table II.

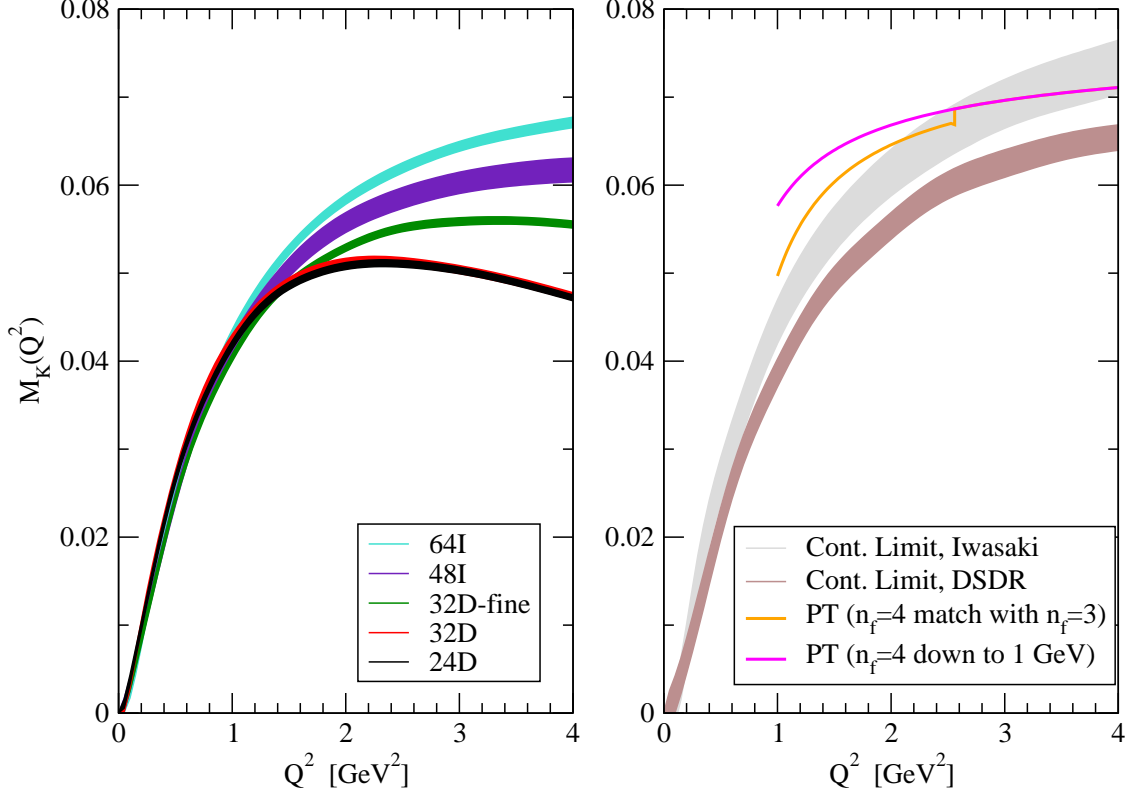


Figure 3. $M_K(Q^2)$ as a function of Q^2 . In the left panel, the lattice results for all five ensembles are given. In the right panel, we have extrapolated the Iwasaki and DSDR results to their continuum limit. The remaining orange and magenta curves are the results from perturbation theory.

After combining the lattice data and perturbative results given in Table II, we have

$$\square_{\gamma W}^{VA} \Big|_{K^0, \text{SU}(3)} = \begin{cases} 2.460(18)_{\text{stat}}(42)_{\text{PT}}(22)_a(1)_{\text{FV}} \times 10^{-3} & Q_{\text{cut}}^2 = 1 \text{ GeV}^2 \\ 2.437(20)_{\text{stat}}(15)_{\text{PT}}(36)_a(1)_{\text{FV}} \times 10^{-3} & Q_{\text{cut}}^2 = 2 \text{ GeV}^2. \\ 2.433(22)_{\text{stat}}(07)_{\text{PT}}(45)_a(1)_{\text{FV}} \times 10^{-3} & Q_{\text{cut}}^2 = 3 \text{ GeV}^2 \end{cases} \quad (15)$$

Here we take the combination of the Iwasaki and perturbative results as the central value and estimate the residual lattice artifacts (with a subscript a) using the discrepancy between Iwasaki and DSDR. The lattice finite-volume effects (with a subscript FV) are estimated by comparing the 24D and 32D results. As a final result, we quote the value of $\square_{\gamma W}^{VA} \Big|_{K^0, \text{SU}(3)}$ at $Q_{\text{cut}}^2 = 2 \text{ GeV}^2$ and add the statistical and systematic errors in quadrature

$$\square_{\gamma W}^{VA} \Big|_{K^0, \text{SU}(3)} = 2.437(44) \times 10^{-3}. \quad (16)$$

Q_{cut}^2	$\square_{\gamma W}^{VA,\leq} _{K^0,\text{SU}(3)}$		$\square_{\gamma W}^{VA,>} _{K^0,\text{SU}(3)}$
	Iwasaki	DSDR	pQCD
1 GeV ²	$0.150(18) \times 10^{-3}$	$0.128(15) \times 10^{-3}$	$2.310(42) \times 10^{-3}$
2 GeV ²	$0.278(20) \times 10^{-3}$	$0.242(16) \times 10^{-3}$	$2.159(15) \times 10^{-3}$
3 GeV ²	$0.371(22) \times 10^{-3}$	$0.326(17) \times 10^{-3}$	$2.062(07) \times 10^{-3}$

Table II. Using the scale Q_{cut}^2 to split the integral range, the contributions of $\square_{\gamma W}^{VA,\leq}|_{K^0,\text{SU}(3)}$ from lattice QCD and $\square_{\gamma W}^{VA,>}|_{K^0,\text{SU}(3)}$ from perturbation theory are shown. For the lattice results, we have performed the continuum extrapolation for Iwasaki and DSDR ensembles separately. For the perturbative results, the central values are compiled using the 4-flavor theory and uncertainties include the higher-loop effects and the higher-twist effects with the error analysis following Ref. [8].

Inserting the result of $\square_{\gamma W}^{VA}|_{K^0,\text{SU}(3)}$ into Eq. (10), we obtain

$$-\frac{8}{3}X_1 + \bar{X}_6^{\text{phys}} = 22.6(1.0) \times 10^{-3} \quad \text{or} \quad -\frac{8}{3}X_1 + \tilde{X}_6^{\text{phys}} = 19.6(1.0) \times 10^{-3}. \quad (17)$$

The previous ChPT analysis [57] quoted the LECs from the minimal resonance model [64, 71] with

$$X_1 = -3.7(3.7) \times 10^{-3}, \quad \tilde{X}_6^{\text{phys}} = 10.4(10.4) \times 10^{-3}. \quad (18)$$

As it is hard to accurately estimate the uncertainty in these LECs from the ChPT perspective, Ref. [57] attributed to them a 100% uncertainty. Combining X_1 and $\tilde{X}_6^{\text{phys}}$ together yields

$$-\frac{8}{3}X_1 + \tilde{X}_6^{\text{phys}} = 20.3(14.3) \times 10^{-3} \quad [\text{minimal resonance model}]. \quad (19)$$

Our result for $-\frac{8}{3}X_1 + \tilde{X}_6^{\text{phys}}$ agrees with the minimal resonance model within few percent. Such a good agreement could easily be fortuitous as the methods used in the two studies are very different and a large uncertainty is assigned to the estimate based on the model.

For the $\pi_{\ell 3}$ decay, substituting the lattice QCD result $\square_{\gamma W}^{VA}|_{\pi} = 2.830(28) \times 10^{-3}$ [8] into Eq. (11) yields

$$\frac{4}{3}X_1 + \bar{X}_6^{\text{phys}} = 14.0(6) \times 10^{-3}. \quad (20)$$

Combining Eqs. (17) and (20) together, we have

$$X_1 = -2.2(4) \times 10^{-3}, \quad \bar{X}_6^{\text{phys}} = 16.9(7) \times 10^{-3}. \quad (21)$$

Here the uncertainty is estimated conservatively through a linear addition. It should be pointed out that in Eq. (21) the estimate of the higher order terms in the ChPT expansion are not included yet.

In ChPT, the RCs δ_K^ℓ have two major sources of theoretical uncertainties: the input of the LECs at $O(e^2p^2)$ and the unknown $O(e^2p^4)$ terms in the ChPT expansion. Using the LECs from this calculation, the former uncertainty is significantly reduced, while the latter one remains. It results in an update of δ_K^ℓ (in units of %)

$$\begin{aligned}
\delta_{K^0}^e &= 0.99(19)_{e^2p^4(11)_{\text{LEC}}} \rightarrow 1.00(19) \\
\delta_{K^0}^\mu &= 1.40(19)_{e^2p^4(11)_{\text{LEC}}} \rightarrow 1.41(19) \\
\delta_{K^\pm}^e &= 0.10(19)_{e^2p^4(16)_{\text{LEC}}} \rightarrow -0.01(19) \\
\delta_{K^\pm}^\mu &= 0.02(19)_{e^2p^4(16)_{\text{LEC}}} \rightarrow -0.09(19).
\end{aligned} \tag{22}$$

We refrain from presenting a corresponding update of $|V_{us}|$ in this paper, because (1) our results for δ_K^ℓ still agree with the existing literature within error bars, and (2) our lattice calculation removes only the LEC uncertainty but not the dominant, $\mathcal{O}(e^2p^4)$ uncertainty. Therefore, we shall instead await a next round of global analysis in the near future such as that in Ref. [11], whose impact on the precision low-energy tests will be more significant. Our lattice result may serve as an important input to such an analysis.

IV. CONCLUSION

Modern-day lattice QCD has reached the era when realistic calculations for many interesting second-order electroweak processes have become feasible. In this work we perform a study of the γW -box correction to the kaon semileptonic decay $\overline{K}^0 \rightarrow \pi^+ e \bar{\nu}_e$. We adopt the new method proposed in Ref. [55], which connects the Sirlin's representation to the ChPT representation in the flavor SU(3) limit. It allows us to determine the LECs for ChPT by computing the axial γW -box correction. We find that the values of the LECs devised from the lattice calculation agree well with the minimal resonance model used in the literature, while a dramatic reduction of the respective uncertainties is achieved. Finally, these LECs are used to estimate the RCs δ_K^ℓ and help to reduce its uncertainty. To further improve the determination of RCs, the inclusion of higher-order terms in ChPT and the lattice QCD computation of the complete set of Feynman diagrams are necessary.

ACKNOWLEDGMENTS

X.F. and L.C.J. gratefully acknowledge many helpful discussions with our colleagues from the RBC-UKQCD Collaborations. X.F. and P.X.M. were supported in part by NSFC of China under Grants No. 11775002 and No. 12070131001 and National Key Research and Development Program of China under Contracts No. 2020YFA0406400. M.G. is supported by EU Horizon 2020 research and innovation programme, STRONG-2020 project, under grant agreement No 824093 and by the German-Mexican research collaboration Grant No. 278017 (CONACyT) and No. SP 778/4-1 (DFG). L.C.J. acknowledges support by DOE Office of Science Early Career Award DE-SC0021147 and DOE grant DE-SC0010339. The work of C.Y.S. is supported in part by the DFG (Project-ID 196253076-TRR 110) and the NSFC (Grant No. 11621131001) through the funds provided to the Sino-German CRC 110 “Symmetries and the Emergence of Structure in QCD”, and also by the Alexander von Humboldt Foundation through the Humboldt Research Fellowship. The computation is performed under the ALCC Program of the US DOE on the Blue Gene/Q (BG/Q) Mira computer at the Argonne Leadership Class Facility, a DOE Office of Science Facility supported under Contract DE-AC02-06CH11357. Computations for this work were carried out in part on facilities of the USQCD Collaboration, which are funded by the Office of Science of the U.S. Department of Energy. The calculation is also carried out on Tianhe 3 prototype at Chinese National Supercomputer Center in Tianjin.

-
- [1] P. A. Zyla *et al.* (Particle Data Group), PTEP **2020**, 083C01 (2020).
 - [2] J. C. Hardy and I. S. Towner, Phys. Rev. **C91**, 025501 (2015), arXiv:1411.5987 [nucl-ex].
 - [3] J. C. Hardy and I. S. Towner, Phys. Rev. C **102**, 045501 (2020).
 - [4] C. Y. Seng, M. Gorchtein, and M. J. Ramsey-Musolf, Phys. Rev. **D100**, 013001 (2019), arXiv:1812.03352 [nucl-th].
 - [5] M. Gorchtein, Phys. Rev. Lett. **123**, 042503 (2019), arXiv:1812.04229 [nucl-th].
 - [6] C.-Y. Seng, M. Gorchtein, H. H. Patel, and M. J. Ramsey-Musolf, Phys. Rev. Lett. **121**, 241804 (2018), arXiv:1807.10197 [hep-ph].
 - [7] M. Tanabashi *et al.* (Particle Data Group), Phys. Rev. **D98**, 030001 (2018).

- [8] X. Feng, M. Gorchtein, L.-C. Jin, P.-X. Ma, and C.-Y. Seng, Phys. Rev. Lett. **124**, 192002 (2020), arXiv:2003.09798 [hep-lat].
- [9] C.-Y. Seng, X. Feng, M. Gorchtein, and L.-C. Jin, Phys. Rev. D **101**, 111301 (2020), arXiv:2003.11264 [hep-ph].
- [10] C.-Y. Seng and U.-G. Meißner, Phys. Rev. Lett. **122**, 211802 (2019), arXiv:1903.07969 [hep-ph].
- [11] M. Antonelli *et al.* (FlaviaNet Working Group on Kaon Decays), Eur. Phys. J. C **69**, 399 (2010), arXiv:1005.2323 [hep-ph].
- [12] M. Moulson, PoS **CKM2016**, 033 (2017), arXiv:1704.04104 [hep-ex].
- [13] P. A. Boyle *et al.* (RBC/UKQCD), JHEP **06**, 164 (2015), arXiv:1504.01692 [hep-lat].
- [14] N. Carrasco, P. Lami, V. Lubicz, L. Riggio, S. Simula, and C. Tarantino, Phys. Rev. D **93**, 114512 (2016), arXiv:1602.04113 [hep-lat].
- [15] S. Aoki, G. Cossu, X. Feng, H. Fukaya, S. Hashimoto, T. Kaneko, J. Noaki, and T. Onogi (JLQCD), Phys. Rev. D **96**, 034501 (2017), arXiv:1705.00884 [hep-lat].
- [16] A. Bazavov *et al.* (Fermilab Lattice, MILC), Phys. Rev. D **99**, 114509 (2019), arXiv:1809.02827 [hep-lat].
- [17] J. Kakazu, K.-i. Ishikawa, N. Ishizuka, Y. Kuramashi, Y. Nakamura, Y. Namekawa, Y. Taniguchi, N. Ukita, T. Yamazaki, and T. Yoshié (PACS), Phys. Rev. D **101**, 094504 (2020), arXiv:1912.13127 [hep-lat].
- [18] S. Aoki *et al.* (Flavour Lattice Averaging Group), Eur. Phys. J. **C80**, 113 (2020), arXiv:1902.08191 [hep-lat].
- [19] W. J. Marciano, Phys. Rev. Lett. **93**, 231803 (2004), arXiv:hep-ph/0402299.
- [20] F. Ambrosino *et al.* (KLOE), Phys. Lett. B **632**, 76 (2006), arXiv:hep-ex/0509045.
- [21] R. J. Dowdall, C. T. H. Davies, G. P. Lepage, and C. McNeile, Phys. Rev. D **88**, 074504 (2013), arXiv:1303.1670 [hep-lat].
- [22] N. Carrasco *et al.*, Phys. Rev. D **91**, 054507 (2015), arXiv:1411.7908 [hep-lat].
- [23] A. Bazavov *et al.*, Phys. Rev. D **98**, 074512 (2018), arXiv:1712.09262 [hep-lat].
- [24] N. Miller *et al.*, Phys. Rev. D **102**, 034507 (2020), arXiv:2005.04795 [hep-lat].
- [25] N. Cabibbo, E. C. Swallow, and R. Winston, Phys. Rev. Lett. **92**, 251803 (2004), arXiv:hep-ph/0307214.
- [26] Y. S. Amhis *et al.* (HFLAV), (2019), arXiv:1909.12524 [hep-ex].

- [27] N. H. Christ, T. Izubuchi, C. T. Sachrajda, A. Soni, and J. Yu (RBC, UKQCD), Phys. Rev. **D88**, 014508 (2013), arXiv:1212.5931 [hep-lat].
- [28] Z. Bai, N. H. Christ, T. Izubuchi, C. T. Sachrajda, A. Soni, and J. Yu, Phys. Rev. Lett. **113**, 112003 (2014), arXiv:1406.0916 [hep-lat].
- [29] N. H. Christ, X. Feng, G. Martinelli, and C. T. Sachrajda, Phys. Rev. D **91**, 114510 (2015), arXiv:1504.01170 [hep-lat].
- [30] N. H. Christ, X. Feng, A. Portelli, and C. T. Sachrajda (RBC, UKQCD), Phys. Rev. D **92**, 094512 (2015), arXiv:1507.03094 [hep-lat].
- [31] N. H. Christ, X. Feng, A. Portelli, and C. T. Sachrajda (RBC, UKQCD), Phys. Rev. D **93**, 114517 (2016), arXiv:1605.04442 [hep-lat].
- [32] N. H. Christ, X. Feng, A. Juttner, A. Lawson, A. Portelli, and C. T. Sachrajda, Phys. Rev. D **94**, 114516 (2016), arXiv:1608.07585 [hep-lat].
- [33] Z. Bai, N. H. Christ, X. Feng, A. Lawson, A. Portelli, and C. T. Sachrajda, Phys. Rev. D **98**, 074509 (2018), arXiv:1806.11520 [hep-lat].
- [34] N. H. Christ, X. Feng, A. Portelli, and C. T. Sachrajda (RBC, UKQCD), Phys. Rev. D **100**, 114506 (2019), arXiv:1910.10644 [hep-lat].
- [35] N. H. Christ, X. Feng, L.-C. Jin, and C. T. Sachrajda, Phys. Rev. D **103**, 014507 (2021), arXiv:2009.08287 [hep-lat].
- [36] B. C. Tiburzi, M. L. Wagman, F. Winter, E. Chang, Z. Davoudi, W. Detmold, K. Orginos, M. J. Savage, and P. E. Shanahan, Phys. Rev. **D96**, 054505 (2017), arXiv:1702.02929 [hep-lat].
- [37] P. E. Shanahan, B. C. Tiburzi, M. L. Wagman, F. Winter, E. Chang, Z. Davoudi, W. Detmold, K. Orginos, and M. J. Savage, Phys. Rev. Lett. **119**, 062003 (2017), arXiv:1701.03456 [hep-lat].
- [38] A. Nicholson *et al.*, Phys. Rev. Lett. **121**, 172501 (2018), arXiv:1805.02634 [nucl-th].
- [39] X. Feng, L.-C. Jin, X.-Y. Tuo, and S.-C. Xia, Phys. Rev. Lett. **122**, 022001 (2019), arXiv:1809.10511 [hep-lat].
- [40] X.-Y. Tuo, X. Feng, and L.-C. Jin, Phys. Rev. **D100**, 094511 (2019), arXiv:1909.13525 [hep-lat].
- [41] W. Detmold and D. J. Murphy (NPLQCD), (2020), arXiv:2004.07404 [hep-lat].
- [42] X. Feng, L.-C. Jin, Z.-Y. Wang, and Z. Zhang, (2020), arXiv:2005.01956 [hep-lat].
- [43] Z. Davoudi and S. V. Kadam, Phys. Rev. D **102**, 114521 (2020), arXiv:2007.15542 [hep-lat].

- [44] Z. Davoudi and S. V. Kadam, (2020), arXiv:2012.02083 [hep-lat].
- [45] M. T. Hansen, H. B. Meyer, and D. Robaina, Phys. Rev. D **96**, 094513 (2017), arXiv:1704.08993 [hep-lat].
- [46] S. Hashimoto, PTEP **2017**, 053B03 (2017), arXiv:1703.01881 [hep-lat].
- [47] P. Gambino and S. Hashimoto, Phys. Rev. Lett. **125**, 032001 (2020), arXiv:2005.13730 [hep-lat].
- [48] N. Carrasco, V. Lubicz, G. Martinelli, C. T. Sachrajda, N. Tantalo, C. Tarantino, and M. Testa, Phys. Rev. **D91**, 074506 (2015), arXiv:1502.00257 [hep-lat].
- [49] V. Lubicz, G. Martinelli, C. T. Sachrajda, F. Sanfilippo, S. Simula, and N. Tantalo, Phys. Rev. **D95**, 034504 (2017), arXiv:1611.08497 [hep-lat].
- [50] D. Giusti, V. Lubicz, G. Martinelli, C. T. Sachrajda, F. Sanfilippo, S. Simula, N. Tantalo, and C. Tarantino, Phys. Rev. Lett. **120**, 072001 (2018), arXiv:1711.06537 [hep-lat].
- [51] X. Feng and L. Jin, Phys. Rev. D **100**, 094509 (2019), arXiv:1812.09817 [hep-lat].
- [52] N. H. Christ, X. Feng, J. Lu-Chang, and C. T. Sachrajda, PoS **LATTICE2019**, 259 (2020).
- [53] A. Desiderio *et al.*, Phys. Rev. D **103**, 014502 (2021), arXiv:2006.05358 [hep-lat].
- [54] R. Frezzotti, M. Garofalo, V. Lubicz, G. Martinelli, C. T. Sachrajda, F. Sanfilippo, S. Simula, and N. Tantalo, (2020), arXiv:2012.02120 [hep-ph].
- [55] C.-Y. Seng, X. Feng, M. Gorchtein, L.-C. Jin, and U.-G. Meißner, JHEP **10**, 179 (2020), arXiv:2009.00459 [hep-lat].
- [56] V. Cirigliano, M. Knecht, H. Neufeld, H. Rupertsberger, and P. Talavera, Eur. Phys. J. C **23**, 121 (2002), arXiv:hep-ph/0110153.
- [57] V. Cirigliano, M. Giannotti, and H. Neufeld, JHEP **11**, 006 (2008), arXiv:0807.4507 [hep-ph].
- [58] A. Sirlin, Rev. Mod. Phys. **50**, 573 (1978), [Erratum: Rev. Mod. Phys.50,905(1978)].
- [59] A. Sirlin, Phys. Rev. **164**, 1767 (1967).
- [60] D. H. Wilkinson and B. E. F. Macefield, Nucl. Phys. **A158**, 110 (1970).
- [61] C.-Y. Seng, D. Galviz, and U.-G. Meißner, JHEP **02**, 069 (2020), arXiv:1910.13208 [hep-ph].
- [62] J. Erler, Rev. Mex. Fis. **50**, 200 (2004), arXiv:hep-ph/0211345 [hep-ph].
- [63] V. Cirigliano, M. Knecht, H. Neufeld, and H. Pichl, Eur. Phys. J. C **27**, 255 (2003), arXiv:hep-ph/0209226.
- [64] S. Descotes-Genon and B. Moussallam, Eur. Phys. J. C **42**, 403 (2005), arXiv:hep-ph/0505077.
- [65] S. A. Larin and J. A. M. Vermaseren, Phys. Lett. **B259**, 345 (1991).

- [66] P. A. Baikov, K. G. Chetyrkin, and J. H. Kuhn, Phys. Rev. Lett. **104**, 132004 (2010), arXiv:1001.3606 [hep-ph].
- [67] Y. Li, S.-C. Xia, X. Feng, L.-C. Jin, and C. Liu, Phys. Rev. D **103**, 014514 (2021), arXiv:2009.01029 [hep-lat].
- [68] W. Detmold, D. J. Murphy, A. V. Pochinsky, M. J. Savage, P. E. Shanahan, and M. L. Wagman, (2019), arXiv:1908.07050 [hep-lat].
- [69] X. Feng, Y. Fu, and L.-C. Jin, Phys. Rev. D **101**, 051502 (2020), arXiv:1911.04064 [hep-lat].
- [70] K. G. Chetyrkin, J. H. Kuhn, and M. Steinhauser, Comput. Phys. Commun. **133**, 43 (2000), arXiv:hep-ph/0004189 [hep-ph].
- [71] B. Ananthanarayan and B. Moussallam, JHEP **06**, 047 (2004), arXiv:hep-ph/0405206.